



# Contactless determination and parametrization of charge-carrier mobility in silicon as a function of injection level and temperature using time-resolved terahertz spectroscopy

Sergio Revuelta  and Enrique Cánovas \**IMDEA Nanociencia, Campus Universitario de Cantoblanco, Faraday 9, 28049 Madrid, Spain*

(Received 22 December 2022; revised 2 February 2023; accepted 3 February 2023; published 23 February 2023)

Here, we analyze, in a noncontact fashion, charge-carrier mobility as a function of injection level and temperature in silicon by time-resolved terahertz spectroscopy (TRTS) and parametrize our data by the classical semiempirical models of Klaassen [*Solid State Electron.* **35**, 953 (1992); *Solid State Electron.* **35**, 961 (1992)] and Dorkel and Leturcq [*Solid State Electron.* **24**, 821 (1981)]. Our experimental results are in very good agreement with the pioneering works of Krausse [*Solid State Electron.* **15**, 1377 (1972)] and Dannhäuser [*Solid State Electron.* **15**, 1371 (1972)], who analyzed these phenomena by employing contact-based methods. This agreement, that validates our methodology, can only be achieved by considering charge-carrier diffusion effects following above band gap near-surface pump photoexcitation of the sample. From our results, obtained over a large range of injection levels, we conclude that the model of Klaassen is the best at describing the collected data at room temperature. Furthermore, we analyze by TRTS the dependence of charge-carrier mobility with temperature for a fixed injection level. Once more, the parametrization made by the classical model of Klaassen describes our data appropriately even without the necessity of applying any fitting parameters (just with the charge-carrier density as an input). In this respect, our work supports the validity of the model and parametrization proposed by Klaassen and illustrates how TRTS can be reliably employed for the quantitative determination of mobility in semiconductors as a function of key parameters such as injection level and temperature.

DOI: [10.1103/PhysRevB.107.085204](https://doi.org/10.1103/PhysRevB.107.085204)

## I. INTRODUCTION

Charge-carrier mobility is a fundamental figure of merit determining the performance of optoelectronic devices. This variable depends critically on few parameters as the charge-carrier concentration via doping, the temperature, and the injection level [1,2]. Pioneering studies of the charge-carrier mobility dependence vs injection level in silicon were made from contact-based techniques [3,4], and these results still represent the basis for semiempirical models employed in modeling charge-carrier mobility as a function of charge-carrier density in silicon [5–9]. These initial studies analyzed the interplay of mobility and injection level by contact-based approaches and hence required the manufacturing of a fully functional working device (e.g., a PIN or PN diode structure).

Over the years all-optical noncontact methods have been employed as alternatives for scrutinizing the charge-carrier mobility–charge-carrier injection relationship, most notably photoconductance decay (PCD) measurements. This technique is very powerful for estimating the mobility, recombination processes, and carrier lifetimes in semiconductors as a function of injection level; however, it cannot disentangle (from conductance) the contributions of carrier density and mobility [10–13] unless it is assisted by a second set of measurements, e.g., time-resolved photoluminescence [13]. Furthermore, PCD techniques can often monitor a relatively narrow range of injection levels (i.e., charge-carrier densities).

A powerful noncontact alternative to PCD is time-resolved terahertz spectroscopy (TRTS) [14–16]. Following an optical pump–terahertz probe scheme, it is possible to retrieve the frequency-resolved complex photoconductivity of a given sample at any pump-probe delay, from which mobility and carrier density can be independently inferred. A TRTS study as a function of impinging—above band gap—pump photon flux, and hence injection level, offers an avenue for determining the interplay between photogenerated charge-carrier density and charge-carrier mobility. Although several studies have already been done using TRTS to analyze the mobility dependence on charge-carrier density in materials such as silicon [17,18], gallium arsenide [19,20], titanium oxide [18], or zinc oxide [21], none of these studies has attempted nor reached a quantitative agreement with classical estimates made by contact methods, a singular aspect that represents by itself a goal between the terahertz and metrology research communities [22].

In this paper, we have employed TRTS to analyze the dependence of the charge-carrier mobility of a sample with injection level and temperature as controlled by photodoping in silicon. From TRTS data at room temperature, we retrieve the expected reduction in the charge-carrier mobility as a function of injection level in a trend that closely matches the one obtained in classical works employing contact-based methods. Notably, this agreement can only be reached by considering diffusion effects impacting the TRTS data and analysis, which we show here can critically play a role on determining unambiguously bulk charge-carrier densities under our TRTS conventional experimental conditions (i.e., near-surface pho-

\*enrique.canovas@imdea.org

toexcitation with ultraviolet photons). Furthermore, we have analyzed the dependence of charge-carrier mobility with temperature at low injection levels and compared our data with the predictions made by the classical semiempirical models of Klaassen [6,7] and Dorkel and Leturcq [5]. Our results, retrieved over a large range of injection levels and temperatures, reveal that the model of Klaassen [6,7] is the best at describing the data at room temperature and as a function of temperature, for the latter variable even without the necessity of applying any fitting parameters (just the charge-carrier density as an input). In this respect, our work supports the validity of the model and parametrization proposed by Klaassen [6,7] and demonstrates that TRTS can be employed as a powerful tool for the quantitative determination of mobility in semiconductors, an aspect validated by the good agreement found between our data and the classical results of Krausse [3] and Dannhäuser [4] by contact methods.

## II. EXPERIMENTAL

The sample analyzed in this paper consisted of a 0.5-mm-thick semi-insulating silicon float zone wafer with  $\langle 100 \rangle$  orientation (Sigma-Aldrich ID: 646687, resistivity = 100–3000  $\Omega$  cm) with native oxide passivation. A Ti : sapphire amplified laser system providing 775 nm wavelength output ( $\sim 150$  fs pulse width at 1 KHz repetition rate) was employed to run the optical pump–terahertz probe experiment [14,18]. For optical pump excitation of the sample, we employed the 387.5 nm output generated by a beta barium borate crystal. The employed  $\sim 1$  THz bandwidth probe was generated via optical rectification on a 1-mm-thick ZnTe crystal cut along the  $\langle 110 \rangle$  axis. The detection of the terahertz beam was performed via electro-optical sampling on a ZnTe crystal of identical characteristics.

In a TRTS measurement, we can monitor the  $\sim 1$  THz width freely propagating probe in the time domain; as such, changes in amplitude and phase induced in the transmitted terahertz probe by the pump excitation can be recorded. From these data, the sheet frequency-resolved complex photoconductivity of the time-dependent sample  $\Delta\sigma_{\text{sheet}}(\omega, t)$  can be retrieved at any pump-probe delay time ( $t$ ). Under the employed photoexcitation conditions (387.5 nm), the optical penetration depth in silicon is estimated to be  $\sim 80$  nm [23], much smaller than the thickness of the sample. This allows us to employ the Tinkham approximation [14,24] from which we can retrieve the frequency-resolved complex photoconductivity as

$$\Delta\sigma_{\text{sheet}}(\omega, t) = \frac{-(n_1 + n_2)}{Z_0} \frac{\Delta E(\omega, t)}{E_{\text{ref}}(\omega)}, \quad (1)$$

where  $Z_0$  is the intrinsic impedance of free space,  $n_1$  is the refractive index of the medium before the sample,  $n_2$  is the refractive index of the photoexcited material,  $E_{\text{ref}}$  is the transmitted terahertz electric field through the unexcited sample, and  $\Delta E$  is the pump-induced change in the terahertz waveform.

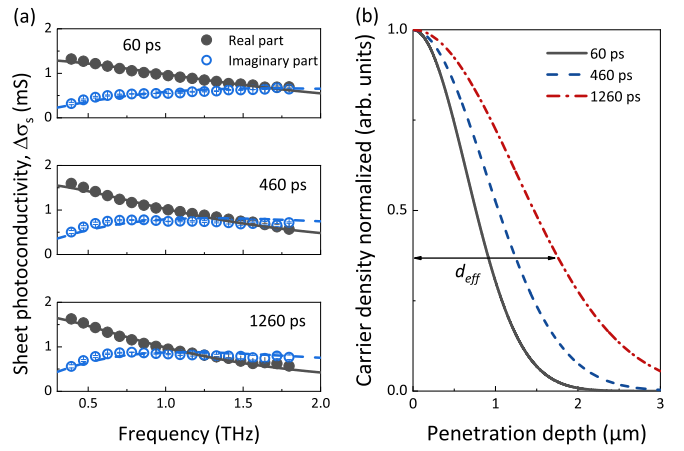


FIG. 1. (a) Complex sheet photoconductivity at 300 K and under 387.5 nm of pump excitation with a fluence of  $10.58 \mu\text{J}/\text{cm}^2$  at different pump-probe delays (60, 460, and 1260 ps). Filled and open symbols refer to the real and imaginary components of the sheet photoconductivity. Solid and dashed lines correspond to the best fit by the Drude model for the real and imaginary components, respectively. (b) Numerical solution for the effective thickness of the photogenerated electron-hole gas for the considered pump-probe delays. The effective thickness for the photoexcited slab is defined as the  $1/e$  drop from the carrier density near the air-solid interface.

## III. RESULTS

In Fig. 1(a), we show the frequency-resolved complex sheet photoconductivity obtained for silicon for three pump-probe delays (from top to bottom: 60, 460, and 1260 ps) at a fluence of  $10.58 \mu\text{J}/\text{cm}^2$  at 387.5 nm of pump wavelength. Black solid and blue open circles are the experimental real and imaginary components of the sheet complex conductivity within the probed terahertz window, respectively. Each plot also shows black solid and blue dashed lines representing, respectively, the best fits to real and imaginary components of the frequency-resolved complex conductivity by using the Drude model as

$$\Delta\hat{\sigma}_{\text{sheet}}(\omega, t) = \Delta\hat{\sigma}_{\text{bulk}}(\omega, t)d = \frac{N_{\text{sheet}}e^2\tau}{m^*(1 - i\omega\tau)}. \quad (2)$$

Here,  $\Delta\hat{\sigma}_{\text{bulk}}(\omega, t)$  represents the complex frequency-resolved bulk photoconductivity,  $d$  is the penetration depth of the impinging photon flux,  $e$  is the electron charge,  $\tau$  is the average scattering time,  $m^*$  is the effective mass, and  $N_{\text{sheet}}$  is the sheet charge-carrier density in units of  $\text{cm}^{-2}$  (i.e.,  $N_{\text{sheet}} = [1-R]N_{hv}$ , where  $R$  and  $N_{hv}$  are the reflectivity and pump photon flux, respectively). From the best Drude fits to the data, we can directly obtain values for the sheet carrier density (by considering an optical effective mass of  $0.16m_e$ )  $N_{\text{sheet}}$  of  $7.97 \times 10^{16}$ ,  $7.55 \times 10^{16}$ , and  $7.08 \times 10^{16} \text{ m}^{-2}$  and averaged scattering times  $\tau$  of 95, 123, and 141 fs, respectively, for the analyzed pump-probe delays of 60, 460, and 1260 ps. These figures show an improvement in scattering rate upon pump-probe delay that has been previously interpreted by some authors as a diffusion process of photogenerated charge carriers from near the surface toward the bulk [20]. In this respect, an increase in scattering rate is linked with a reduction in bulk charge-carrier density of the electron-hole plasma as

modulated by a time-dependent penetration depth. Then  $d$  in Eq. (2) should be defined as  $d_{\text{eff}}(t)$  [see Fig. 1(b), where  $d_{\text{eff}}(t)$  represents the distance from the surface of the sample where the initial carrier density amplitude drops a value of  $1/e$ ].

Right after charge-carrier photogeneration [ $d_{\text{eff}}(t \sim 0)$ ], the penetration depth for the photoexcited slab in silicon is estimated to be  $\sim 80$  nm [23] under the 387.5 nm above band gap pump beam. As neither hot carrier cooling [25], nor charge-carrier surface/bulk recombination substantially affect our dynamics within the analyzed  $\sim 1$  ns probed time window (see Fig. S2 in the Supplemental Material [26]), we can find a numerical solution for the effective time-dependent thickness  $d_{\text{eff}}(t)$  of the expanding electron-hole plasma following the expression  $n(x, t) = (N_0/\sqrt{4\pi D_{ab}t})\exp(-x^2/4D_{ab}t)$ , where  $N_0$  refers to the initial carrier density, and  $D_{ab}$  is the ambipolar diffusivity in silicon [27,28]. The ambipolar diffusivity is parametrized with the scattering time of the electron-hole plasma retrieved from the frequency-resolved complex sheet photoconductivity (see Eq. (S2) in the Supplemental Material [26]).

Once the effective penetration depth is accurately estimated, we can obtain the bulk photoconductivity of the sample as  $\Delta\hat{\sigma}(\omega, t) = \Delta\hat{\sigma}_{\text{sheet}}(\omega, t)/d_{\text{eff}}(t)$ . Analogously, we can obtain the bulk carrier density as a function of time as  $N_{\text{bulk}}(t) = N_{\text{sheet}}/d_{\text{eff}}(t)$ , which corresponds to the photoinjected density of charge carriers. From the results shown in Fig. 1(a), we retrieve charge-carrier concentrations of  $(2.0 \pm 0.3) \times 10^{17}$ ,  $(6.6 \pm 1.4) \times 10^{16}$ , and  $(3.5 \pm 0.5) \times 10^{16} \text{ cm}^{-3}$  and charge-carrier mobilities of  $640 \pm 22$ ,  $831 \pm 43$ , and  $956 \pm 38 \text{ cm}^2 \text{ V}^{-1} \text{ s}^{-1}$  for the pump-probe delays of 60, 460, and 1260 ps, respectively (notice here that mobility is defined as  $\mu[N_{\text{bulk}}] = e\tau[N_{\text{bulk}}]/m^*$ ).

To infer the variation of charge-carrier mobility vs injection level, we performed TRTS experiments for a broad range of 387.5 nm pump excitation conditions ranging between  $\sim 0.15$  and  $\sim 70 \mu\text{J}/\text{cm}^2$  and at pump-probe delays  $> 10$  ps, thereby ensuring the complete cooling of hot carriers [25] (see Fig. S3 in the Supplemental Material [26]). The employed upper threshold photon flux was simply limited by our setup specs. For small photoexcitation conditions (below  $\sim 1 \mu\text{J}/\text{cm}^2$ ), the recorded frequency-resolved complex photoconductivity was found to be invariant vs photon flux and pump-probe delay. Beyond this threshold, an increase in photon flux alone for a given pump-probe delay was sufficient to modulate the charge-carrier scattering rate, in good agreement with a previous TRTS study made in silicon [18]. Furthermore, for each given fluence above the mentioned threshold of  $\sim 1 \mu\text{J}/\text{cm}^2$ , we found the same temporal trend shown in Fig. 1, i.e., an improvement in charge-carrier scattering rate as a function of pump-probe delay. Considering diffusion processes for each analyzed fluence (and pump-probe delay), an accurate bulk carrier density can be inferred and linked to the obtained scattering rate from TRTS analysis. In agreement with a previous study conducted in GaAs which considered diffusion effects following photoexcitation [20], we found a substantial overlap between the data obtained from different optical pump-terahertz probe measurements made at different pump fluences (Fig. 2(a) and Table S3 in the Supplemental Material [26]), an aspect that supports the validity for the diffusion model depicted in Fig. 1(b). Figure 2(b) summarizes our

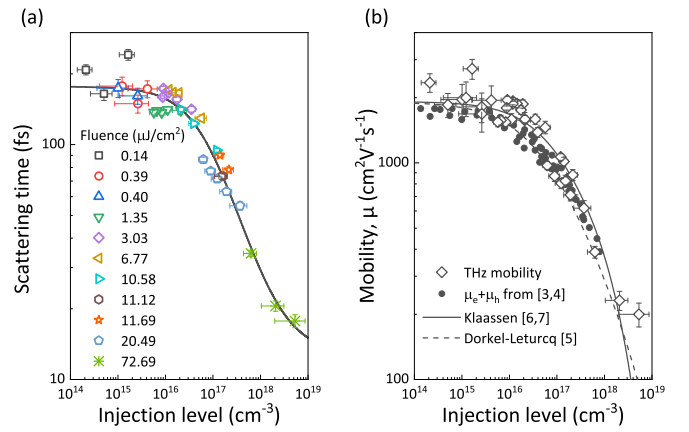


FIG. 2. (a) Scattering time as function of injection level. Different symbols correspond to different fluences as indicated. Solid line is the best fit to a hyperbolic function as described in the text. (b) Room temperature charge-carrier mobility as function of injection level. Open diamonds refer to experimental points retrieved from time-resolved terahertz spectroscopy (TRTS). Black solid dots correspond to the charge-carrier mobility measured by Krausse [3] and Dannhäuser [4]. Solid dashed line indicates the theoretical value predicted by Dorkel and Leturcq [5], while solid line corresponds to the model described by Klaassen [6,7].

findings as open diamonds regarding charge-carrier mobility vs injection level. From the figure, injection level modulates charge-carrier mobility in the sample for carrier concentrations above  $\sim 10^{16} \text{ cm}^{-3}$ . In Fig. 2(b), we also include as solid circles the classical data obtained by Krausse [3] and Dannhäuser [4], representing the sum mobility ( $\mu_e + \mu_h$ ) as a function of injection level measured by contact-based methods on working devices. Remarkably, the optically retrieved terahertz mobility as a function of photoinduced carrier density agrees quite well with the electrical carrier mobility obtained via contact methods. Here, this correlation is made by TRTS and over a large range of injection levels ( $> 1 \times 10^{16} \text{ cm}^{-3}$ ) when compared with, e.g., photoconductance-based noncontact methods [13,29]. We warn the reader that this agreement between TRTS data and the one obtained by contact methods is only reached if diffusion of photogenerated charge carriers from the surface toward the bulk is considered; otherwise, bulk charge-carrier densities are strongly overestimated (see Supplemental Material Fig. S4 [26]).

To parametrize the observed experimental results summarized in Fig. 2(b), we fit the data by the classical models developed by Dorkel and Leturcq [5] (dashed line) and Klaassen [6,7] (solid line). In brief, the Dorkel and Leturcq [5] approach considers the mobility contributed by phonon-carrier, impurity-carrier, and carrier-carrier interactions. On the other hand, the Klaassen [6,7] model employs a more refined model by considering phonon-carrier and electron-hole interactions and effects of the majority and minority impurity scattering while including a screening effect and an increase of the system temperature with charge-carrier density. A summary of the parameters employed in the models can be found in Tables S1 and S2 in the Supplemental Material [26]. From our results, we can conclude that the Klaassen [6,7] model offers a better description of the experimental

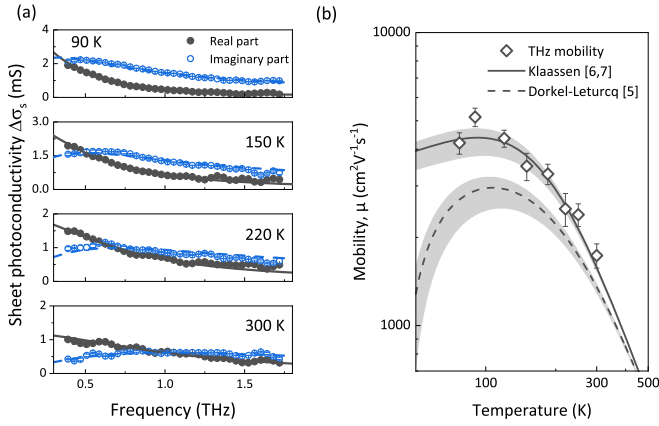


FIG. 3. (a) Complex sheet photoconductivity for silicon measured with different temperatures at a fluence of  $1.55 \mu\text{J}/\text{cm}^2$  and fixed pump-probe delay of 1 ns. Filled and open symbols refer to the real and imaginary components of the sheet photoconductivity. Solid and dashed lines represent the best fit of the Drude model for the real and imaginary parts, respectively. (b) Temperature dependence on charge-carrier mobility retrieved from the signatures of the frequency-resolved photoconductivity. Open black symbols refer to experimental points, while the solid dashed line indicates the carrier mobility predicted by Dorkel and Leturcq [5], and the solid line corresponds to the model described by Klaassen [6,7]. The gray areas represent the lower and maximum error deviations on the average inferred charge-carrier density within the analyzed range of temperatures.

data retrieved by TRTS, a conclusion that agrees with non-contact PCD data collected over a narrower injection level window [9,13,29]. At present, we cannot rationalize the slight deviation between TRTS data and those retrieved by contact methods for concentrations  $> 1 \times 10^{16} \text{ cm}^{-3}$ ; in this respect, Klaassen [6] suggests that these data might be underestimated by an increase of temperature in the system during the measurements.

Once we have analyzed the dependence of the mobility vs injection level by TRTS at room temperature, we study the dependence of the mobility as a function of temperature for a fixed sheet charge-carrier injection. To study this dependence, we selected a photon flux of  $\sim 1.55 \mu\text{J}/\text{cm}^2$ , low enough to prevent strong diffusion effects in the samples. Figure 3 shows exemplary measurements of the frequency-resolved complex sheet photoconductivity under 387.5 nm excitation at 1 ns of pump-probe delay and different temperatures: 90, 150, 220, and 300 K. All the plots can be properly described by the Drude model. Considering a temperature-dependent ambipolar diffusivity (see Fig. S1 in the Supplemental Material [26]), we estimate charge-carrier densities of  $(1.98 \pm 0.13) \times 10^{16}$ ,  $(1.88 \pm 0.23) \times 10^{16}$ ,  $(1.57 \pm 0.27) \times 10^{16}$ , and  $(1.44 \pm 0.21) \times 10^{16} \text{ cm}^{-3}$  which are linked to charge-carrier mobilities of  $5149 \pm 373$ ,  $3499 \pm 373$ ,  $2501 \pm 322$ , and  $1735 \pm 164 \text{ cm}^2 \text{ V}^{-1} \text{ s}^{-1}$ , respectively, for the abovementioned temperatures. As anticipated by the selection of the low photon flux, the carrier concentration values are almost identical as a function of temperature, ranging from  $\sim 2 \times 10^{16}$  to  $\sim 1.4 \times 10^{16} \text{ cm}^{-3}$ ;

this aspect is critical for parametrizing the collected mobility data for a fixed carrier concentration. In this sense, the obtained variation of mobility vs  $T$ , truly represents the impact of temperature on the monitored scattering rates for a given charge-carrier injection. Figure 3(b) summarizes, as open diamonds, the charge-carrier mobility inferred from TRTS analysis for a set of temperatures ranging between 77 and 300 K ( $1.55 \mu\text{J}/\text{cm}^2$ , 387.5 nm and 1 ns of pump-probe delay, see Fig. S5 in the Supplemental Material [26] for the rest of the frequency-resolved data). Figure 3(b) also includes a parametrization of the obtained data following the models of Klaassen [6,7] (solid line) and Dorkel and Leturcq [5] (dashed lines), where remarkably the only variable input is the charge-carrier concentration figure of  $1.73 \times 10^{16} \text{ cm}^{-3}$  (i.e., the median value of the retrieved carrier densities from the Drude fits). It is evident from the plot that the mobility inferred by TRTS matches nicely the curve predicted by Klaassen [6,7], while the Dorkel and Leturcq [5] model cannot correctly describe the experimental data.

The validation made here for the Klaassen [6,7] model as a function of temperature for a given injection level is unique. A couple of PCD works have previously attempted such a study. In these works, authors [9,29] found that the Klaassen [6,7] model failed to describe the experimentally resolved trend for temperatures below  $\sim 150$  K. The reason for this disagreement is unclear to us; however, we note that, for low temperatures, one should consider an extra effect decreasing charge-carrier density in silicon, an effect linked to the condensation of photogenerated  $e-h$  pairs into excitons. This effect indeed has previously been reported and modeled to occur at temperatures  $\sim 100$  K onset [30–32].

#### IV. CONCLUSIONS

In this paper, we have investigated the dependence of the charge-carrier mobility vs injection density and temperature in silicon using TRTS. Our results agree well with previously reported studies in silicon measured by contact methods [3,4] and validate the semiempirical model developed by Klaassen [6,7]. Notably, the agreement with previous data and modeling can only be achieved when charge-carrier diffusion effects following near-surface photoexcitation are considered. Otherwise, the charge-carrier density may be overestimated for a given charge-carrier mobility. The retrieved dependency of the carrier mobility for a fixed injection level with temperature further supports the validity of the Klaassen [6,7] model against the one proposed by Dorkel and Leturcq [5].

While in principle our approach can be generalized to any semiconductor, surface recombination effects might complicate or make determining unambiguously charge-carrier density as a function of time after excitation impossible. Furthermore, a preknowledge of the diffusion constant vs injection and temperature seems required for properly modeling the retrieved TRTS data. Nevertheless, our results highlight the strength of TRTS as a powerful noncontact method for analyzing the mobility in semiconductors as a function of key variables such as the injection level and temperature.

## ACKNOWLEDGMENTS

We acknowledge financial support from Grants No. PID2019-107808RA-I00 and No. TED2021-129624B-C44 funded by MCIN/AEI/10.13039/501100011033

and by “NextGenerationEU”/PRTR. We also acknowledge financial support from the Comunidad de Madrid through Projects No. 2017-T1/AMB-5207 and No. 2021-5A/AMB-20942.

- [1] C. Jacoboni, C. Canali, G. Ottaviani, and A. Alberigi Quaranta, A review of some charge transport properties of silicon, *Solid State Electron.* **20**, 77 (1977).
- [2] K. W. Böer and U. W. Pohl, *Semiconductor Physics* (Springer, Cham, 2018).
- [3] J. Krausse, Die Abhängigkeit der Trägerbeweglichkeit in Silizium von der Konzentration der freien Ladungsträger—II, *Solid State Electron.* **15**, 1377 (1972).
- [4] F. Dannhäuser, Die Abhängigkeit der Trägerbeweglichkeit in Silizium von der Konzentration der freien Ladungsträger—I, *Solid State Electron.* **15**, 1371 (1972).
- [5] J. M. Dorkel and P. Leturcq, Carrier mobilities in silicon semi-empirically related to temperature, doping and injection level, *Solid State Electron.* **24**, 821 (1981).
- [6] D. B. M. Klaassen, A unified mobility model for device simulation—I. Model equations and concentration dependence, *Solid State Electron.* **35**, 953 (1992).
- [7] D. B. M. Klaassen, A unified mobility model for device simulation—II. Temperature dependence of carrier mobility and lifetime, *Solid State Electron.* **35**, 961 (1992).
- [8] Y. Agrahari and A. K. Dutta, An empirical model for bulk electron mobility in Si at cryogenic temperatures, *Silicon* **15**, 563 (2023).
- [9] P. Zheng, F. E. Rougieux, D. MacDonald, and A. Cuevas, Measurement and parameterization of carrier mobility sum in silicon as a function of doping, temperature and injection level, *IEEE J. Photovoltaics* **4**, 560 (2014).
- [10] R. A. Sinton and A. Cuevas, Contactless determination of current-voltage characteristics and minority-carrier lifetimes in semiconductors from quasi-steady-state photoconductance data, *Appl. Phys. Lett.* **69**, 2510 (1996).
- [11] R. A. Sinton, S. Consulting, S. Jose, A. Cuevas, and M. Stuckings, Quasi-steady-state photoconductance, a new method for solar cell material and device characterization, in *Conference Record of the Twenty Fifth IEEE Photovoltaic Specialists Conference* (IEEE, 1996), p. 457.
- [12] M. Goodarzi, R. Sinton, D. Chung, B. Mitchell, T. Trupke, and D. Macdonald, A comparison between quasi-steady state and transient photoconductance lifetimes in silicon ingots: Simulations and measurements, in *IEEE 44th Photovoltaic Specialist Conference (PVSC)* (IEEE, 2017), p. 2707.
- [13] Z. Hameiri, F. Rougieux, R. Sinton, and T. Trupke, Contactless determination of the carrier mobility sum in silicon wafers using combined photoluminescence and photoconductance measurements, *Appl. Phys. Lett.* **104**, 073506 (2014).
- [14] R. Ulbricht, E. Hendry, J. Shan, T. F. Heinz, and M. Bonn, Carrier dynamics in semiconductors studied with time-resolved terahertz spectroscopy, *Rev. Mod. Phys.* **83**, 543 (2011).
- [15] P. Kužel and H. Němec, Terahertz spectroscopy of nanomaterials: A close look at charge-carrier transport, *Adv. Opt. Mater.* **8**, 1900623 (2020).
- [16] C. A. Schmuttenmaer, Exploring dynamics in the far-infrared with terahertz spectroscopy, *Chem. Rev.* **104**, 1759 (2004).
- [17] T. Terashige, H. Yada, Y. Matsui, T. Miyamoto, N. Kida, and H. Okamoto, Temperature and carrier-density dependence of electron-hole scattering in silicon investigated by optical-pump terahertz-probe spectroscopy, *Phys. Rev. B* **91**, 241201(R) (2015).
- [18] E. Hendry, M. Koeberg, J. Pijpers, and M. Bonn, Reduction of carrier mobility in semiconductors caused by charge-charge interactions, *Phys. Rev. B* **75**, 233202 (2007).
- [19] M. C. Beard, G. M. Turner, and C. A. Schmuttenmaer, Transient photoconductivity in GaAs as measured by time-resolved terahertz spectroscopy, *Phys. Rev. B* **62**, 15764 (2000).
- [20] Z. Mics, A. D’Angio, S. A. Jensen, M. Bonn, and D. Turchinovich, Density-dependent electron scattering in photoexcited GaAs in strongly diffusive regime, *Appl. Phys. Lett.* **102**, 231120 (2013).
- [21] E. Hendry, M. Koeberg, and M. Bonn, Exciton and electron-hole plasma formation dynamics in ZnO, *Phys. Rev. B* **76**, 045214 (2007).
- [22] Brian G. Alberding, W. Robert Thurber, and Edwin J. Heilweil, Direct comparison of time-resolved terahertz spectroscopy and Hall Van der Pauw methods for measurement of carrier conductivity and mobility in bulk semiconductors, *J. Opt. Soc. Am. B: Opt. Phys.* **34**, 1392 (2017).
- [23] G. de Graaf and R. F. Wolffenbuttel, Illumination source identification using a CMOS optical microsystem, *IEEE Trans. Instrum. Meas.* **53**, 238 (2004).
- [24] J. Neu and C. A. Schmuttenmaer, Tutorial: An introduction to terahertz time domain spectroscopy (THz-TDS), *J. Appl. Phys.* **124**, 231101 (2018).
- [25] H. Tanimura, J. Kanasaki, K. Tanimura, J. Sjakste, and N. Vast, Ultrafast relaxation dynamics of highly excited hot electrons in silicon, *Phys. Rev. B* **100**, 035201 (2019).
- [26] See Supplemental Material at <https://link.aps.org/supplemental/10.1103/PhysRevB.107.085204> for additional experimental data and detailed description of models.
- [27] H. Zhao, Temperature dependence of ambipolar diffusion in silicon on insulator, *Appl. Phys. Lett.* **92**, 112104 (2008).
- [28] M. Rosling, H. Bleichner, P. Jonsson, and E. Nordlander, The ambipolar diffusion coefficient in silicon: Dependence on excess-carrier concentration and temperature, *J. Appl. Phys.* **76**, 2855 (1994).
- [29] F. E. Rougieux, P. Zheng, M. Thiboust, J. Tan, N. E. Grant, D. H. MacDonald, and A. Cuevas, A contactless method for determining the carrier mobility sum in silicon wafers, *IEEE J. Photovoltaics* **2**, 41 (2012).
- [30] T. Suzuki and R. Shimano, Exciton Mott Transition in Si Revealed by Terahertz Spectroscopy, *Phys. Rev. Lett.* **109**, 046402 (2012).

[31] T. Suzuki and R. Shimano, Time-Resolved Formation of Excitons and Electron-Hole Droplets in Si Studied Using Terahertz Spectroscopy, *Phys. Rev. Lett.* **103**, 057401 (2009).

[32] T. Suzuki and R. Shimano, Cooling dynamics of photoexcited carriers in Si studied using optical pump and terahertz probe spectroscopy, *Phys. Rev. B* **83**, 085207 (2011).